Petroleum Science 23 (2026) 1543–1552

Contents lists available at ScienceDirect

Petroleum Science

journal homepage: www.keaipublishing.com/en/journals/petroleum-science

Original Paper

Degradable PAM hydrogel mediated by hydroxy acids for temporary plugging

Ren-Jing Ji [a], Xiao-Rong Yu [a,b,*], Zhi-Xiang Xu [c], Xian-Qun Wang [a], Jia-Yu Tan [a], Yong-Quan Han [d], Huan Yang [a,b], Gao-Shen Su [a,b]

[a] College of Chemistry and Environmental Engineering, Yangtze University, Jingzhou, 434023, Hubei, China
[b] Hubei Engineering Research Centers for Clean Production and Pollution Control of Oil and Gas Fields, Jingzhou, 434023, Hubei, China
[c] School of Energy and Power Engineering, Jiangsu University, Zhenjiang, 212013, Jiangsu, China
[d] The No.9 Production Plant of Changqing Oilfield Company, CNPC, Yinchuan, 750000, Ningxia, China

ARTICLE INFO

Article history:
Received 11 January 2025
Received in revised form
11 July 2025
Accepted 6 December 2025
Available online 11 December 2025

Edited by Min Li

Keywords:
Temporary plugging
Self-degradable gel plug
Controlled degradation
Hydroxy acid
Pressure resistance performance

ABSTRACT

In this study, the degradation time of gel plugs was regulated by introducing hydroxy acids to adjust the crosslink density, effectively addressing the challenge of controllable degradation time in existing gel plugs. The degradation time of the self-degradable gel plug (SDGP) was extended from 53 h without acid to 235 h with the addition of tartaric acid. Notably, the introduction of hydroxy acids not only regulated the degradation time of the SDGP but also enhanced its properties. The breakthrough pressure of the SDGP without acid was 0.53 MPa, while that of the SDGP with citric acid was 0.74 MPa. Additionally, self-degradation of the SDGP could be achieved after maintaining high strength for a period, ultimately degrading to a liquid with a viscosity of less than 200 mPa·s. The introduction of hydroxy acids increased the crosslinking density between polymer chains and reduced the internal free water content, thereby slowing the hydrolysis of ester groups to achieve controlled degradation of the SDGP. Furthermore, when the crosslinker poly(ethylene glycol) diacrylate was hydrolyzed, the hydroxy acids acted as a crosslinker to re-crosslink the polymer chains, with both the hydroxyl and carboxyl groups in the hydroxy acids participating simultaneously. This study provides a novel approach to adjusting crosslink density to regulate the degradation time of temporary plugging polymer gels, which avoids subsequent gel-breaking operations, reduces costs, and simplifies the operation process.

1. Introduction

With the increasing depth of oil and gas exploitation, pressurized operations have become widely utilized in drilling and well workover processes (Mardashov et al., 2021; Shu et al., 2023). In pressurized operations, high-density kill fluids and casing valves are often employed to control pressure. However, kill fluids can occasionally contaminate the formation, while casing valves are expensive and susceptible to failure under complex well conditions (Chen et al., 2012). In recent years, researchers have investigated the application of polymer gels for pressure control (Jia et al., 2020; Xu et al., 2024; Yin et al., 2022; Zhou et al., 2025; Ziad et al., 2016). Bai et al. (2022) developed a polymer gel designed for pressure control in high-pressure gas reservoirs. This gel exhibits exceptional well kill capacity, achieving a peak performance of 8.8 MPa/100 m after aging at 160 °C. Ying et al. (2021) introduced a gel-plug system for temporary pressure blocking, ensuring that no gas, pressure, or liquid remains in the open well after the well kill operation. The fundamental principle of using polymer gels for pressure control involves injecting the raw material into the wellbore, where it crosslinks at the targeted location to form a gel plug with high strength and viscoelasticity, effectively sealing formation pressure (Kang et al., 2024; Li et al., 2020). Compared to casing valves, the operational depth of the gel plug is more flexible. Moreover, employing a gel plug for pressure control offers advantages including simple construction and low cost (Jia et al., 2021). Upon completion of the controlled pressure operation, the gel plug must be broken. The process of breaking the gel is

* Corresponding author.
E-mail address: yxr_cjdx@163.com (X.-R. Yu).
Peer review under the responsibility of China University of Petroleum (Beijing).

https://doi.org/10.1016/j.petsci.2025.12.014

crucial to restoring the formation pressure. Li et al. (2018) developed an H_2S-resistant gel plug that can be broken down using hydrogen peroxide and potassium permanganate. Cheng et al. (2022) prepared a gel plug for the temporary isolation of bare wells, which was completely degraded by injecting a high concentration of ammonium persulfate. However, ammonium persulfate, hydrogen peroxide, and potassium permanganate, which are strong oxidative gel breaker, tend to corrode the wellbore and casing (Kang et al., 2023; Xu et al., 2023).

Based on the existing challenges associated with oxidative gel breakers, numerous researchers have focused on the development of degradable gels (Burni et al., 2024; Liu et al., 2023; Yang et al., 2024b, 2024a). Wang et al. (2022) synthesized a self-degradable gel with high adhesion using acrylamide (AM), acrylic acid (AA), and 2,2-dimethylpropane-1,3-diyl diacrylate. This gel formulation eliminated the need for additional gel breaker injections after the completion of pressure control operations. Similarly, Ji et al. (2024) prepared a self-degradable gel plug synthesized using AM and N,N′-butyl bis[(2-acryloyloxyethyl)ethyl dimethyl ammonium bromide]. They modulated the crosslink density by varying the concentration of the crosslinker, enabling controlled regulation of the degradation time. In these studies, researchers employed degradable crosslinkers to formulate degradable gels. Following gelation, hydrolysis of the ester groups in degradable crosslinkers results in the gradual breakdown of crosslinking points, which subsequently disrupts the polymer network structure and facilitates gel degradation. The degradation time of the gel can be adjusted by altering the concentration of the crosslinker. However, modifying the crosslinker concentration impacts the gel's properties, including strength, toughness, and adhesion (Song et al., 2023). Consequently, achieving controllable regulation of degradation time without compromising the mechanical properties of the gel remains a critical challenge (Wang et al., 2024). Currently, hydroxy acids are widely utilized in oilfields as green biomaterials (Liu et al., 2010; Ramanathan and Nasr-El-Din, 2021; Yang et al., 2023). In degradable crosslinkers, the hydrolysis of ester groups produces hydroxyl and carboxyl groups on the polymer chain. The unique structure of hydroxy acids, which incorporates both hydroxyl and carboxyl functional groups, presents opportunities for re-crosslinking the polymer chain.

To assess the potential of hydroxy acids in modulating the degradation time of gel plugs, this study aims to achieve the following objectives: to prepare a self-degradable gel plug, to investigate the role of hydroxy acids in controlling its degradation time, and to analyze the underlying mechanisms involved.

2. Materials and methods

2.1. Materials

Poly(ethyleneglycol) diacrylate (PEGDA, Mn: 600), Shanghai Aladdin Biochemical Science and Technology Co. Ltd.; acrylamide (AM, ≥98.0%), citric acid (≥99.8%), tartaric acid (≥99.5%), lactic acid (AR), ammonium persulfate (APS, ≥98.0%), Sinopharm Chemical Reagent Co., Ltd.; deionized water, made in the laboratory.

2.2. Preparation of the SDGP

A total of 8 g of AM, 0.3 g of PEGDA, and 0.3 mmol of hydroxy acids were added to a reagent bottle, while the control group did not include hydroxy acids. Subsequently, 1 mL of a 2 wt% APS solution was added, and the solution was adjusted to a total weight of 100 g with deionized water. The bottles were then sealed and placed in an oven at 90 °C for polymerization. Once the solution lost its fluidity, a self-degradable gel plug was obtained. The synthesis equation of SDGP is illustrated in Fig. 1(a).

2.3. Characterization and performance evaluation methods

2.3.1. Characterization testing of SDGP

The functional groups of SDGP were characterized using a Nicolet 6700 Fourier Transform Infrared Spectrometer (FTIR, Thermo Scientific, USA). The scanning wavenumber range was 4000 to 500 cm^{-1}, with 16 scans conducted at a resolution of 4 cm^{-1}. SDGP samples were cut and dried in an oven at 50 °C until a constant mass was achieved. Subsequently, the SDGP was further cut into smaller pieces and frozen in liquid nitrogen to prepare test samples. The thermal stability of these samples was assessed using a Labsys evo Thermogravimetric Analyzer (TG, Setaram, France), which was heated from 50 to 600 °C in a nitrogen atmosphere at a rate of 10 °C/min, while maintaining a nitrogen flow rate of 80 mL/min. The samples were secured on the stage with conductive adhesive. Prior to observation, the surface of the samples was coated with gold using an ion sputtering apparatus (Beijing Yulong Times Technology Co., Ltd., China) to enhance conductivity. Scanning Electron Microscopy (SEM, TESCAN, CZ) was used to observe the surface morphology of the gel plugs, which were examined with an accelerating voltage of 10 kV. The transverse relaxation time (T_2) of SDGP at room temperature was determined using the Carr-Purcell-Meiboom-Gill sequence of a low-field nuclear magnetic resonator (LF-NMR, Suzhou Newmark Analytical Instruments Co., Ltd., China). The acquired CPMG exponential decay curve was inverted with the MultiExpInv Analysis software of the instrument to obtain the T_2 map. The main parameters were set to: SF = 22 MHz, O_1 = 100938.28 Hz, P_1 = 2.72 μs, P_2 = 5.52 μs, TW = 6500 ms, SW = 200 kHz, RFD = 0.08 ms, NS = 4, TE = 0.9 ms, NECH = 18,000. The crystallinity of the self-degrading gel plugs was evaluated by X-ray diffractometer (XRD, Shimadzu, Japan).

2.3.2. Performance evaluation of SDGP

(1) Measurement of gelation time and degradation time

The reagent bottles were inverted to observe the fluidity of the gel plug surfaces (Sydansk, 1990). Fig. 1(b) illustrates the various flow states of the gel plugs, where state A represents no flow, and state D represents a fully flowing condition. In this paper, the duration for the gel plug to lose its fluidity (transitioning to state A) is defined as the gelation time. Conversely, the duration for the gel plug to regain its fluidity (transitioning to state D) after gelation is defined as the degradation time.

(2) Tensile experiment

The base solution of SDGP was injected into dumbbell-shaped molds to produce gel sheets measuring 115 mm in length, 4 mm in width, and 2 mm in thickness. Tensile experiments were conducted using an electronic tensile tester (Jinan Xinguang Testing Machine Manufacturing Co., Ltd., China) at a rate of 10 mm/min. The elongation at break was calculated as shown in Eq. (1).

$$\delta = (L - L_0) / L_0 \tag{1}$$

In Eq. (1): δ is the elongation at break; L_0 is the original marking distance of the sample, mm; L is the distance between the marking lines when the sample breaks, mm.

The tensile stress of SDGP were calculated as shown in Eq. (2).

$$\sigma = F/ah \tag{2}$$

In Eq. (2), σ is the tensile stress, MPa; F is the maximum tensile force, N; a is the sample width, mm; and h is the sample thickness, mm.

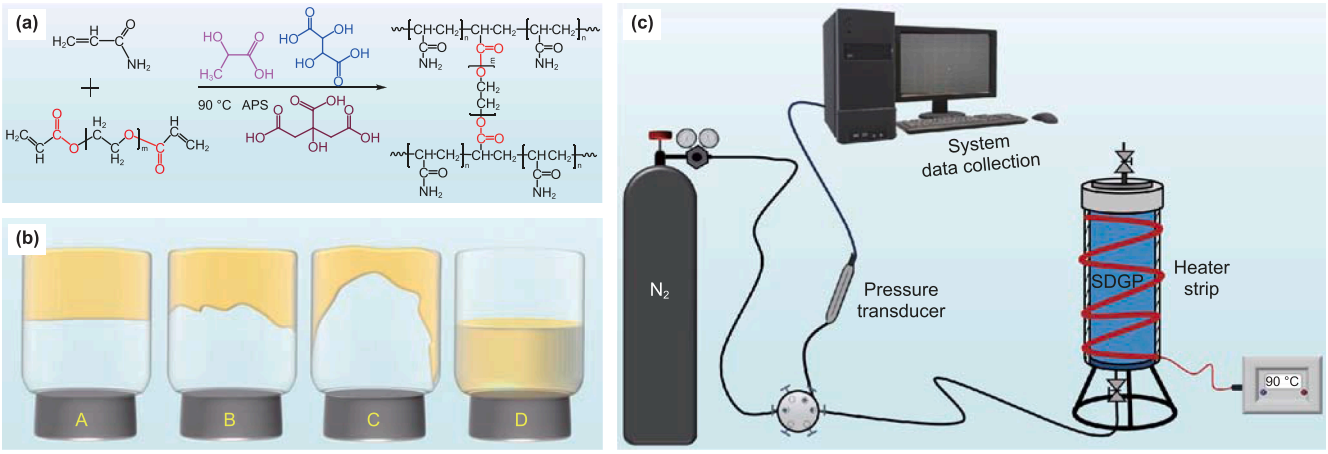

Fig. 1. **(a)** Equation for the synthesis of SDGP, **(b)** schematic diagram of the different fluidity of SDGP, **(c)** pressure resistance performance evaluation device of SDGP.

(3) Pressure resistance measurement

The pressure resistance of SDGP was evaluated using a pressurized test apparatus (Ji et al., 2024) as depicted in Fig. 1(c). Initially, raw material liquid was prepared and injected into the simulated tube column (1 m in length, 0.127 m in diameter) for the test. The gel plugs within the column were heated according to a programmed schedule, after which nitrogen was released from the bottom of the column to continuously apply pressure until the maximum pressure, known as the breakthrough pressure, was attained. This maximum pressure at this point represented the pressure-bearing strength of the self-degradable gel plugs.

(4) Measurement of viscosity of residual liquid after degradation of SDGP

The viscosity of residual liquid was measured using a viscometer (Brookfield, USA) at a temperature of 90 °C. The residual liquid was injected into a cylindrical sample cup, after which the rotor was inserted into the sample. The testing commenced once the temperature within the sample cup stabilized at 90 °C, utilizing the SC4-21 rotor at a speed of 5 rpm.

3. Results and discussion

3.1. Characterization analysis of SDGP

Fig. 2(a) illustrates the FTIR spectra of four SDGP samples. Notably, the band at 3423 cm^{-1} corresponds to the O–H bond stretching vibration absorption bands in hydroxy acids, while the band at 3195 cm^{-1} is N–H band stretching vibration absorption bands in primary amides (Du et al., 2025). The bands at 2931 and 2861 cm^{-1} are stretching vibration absorption bands of methylene C–H (Wang et al., 2022). Additionally, the band at 1660 cm^{-1} signifies the stretching vibration of the C=O bond, and the band at 1608 cm^{-1} is the deformation vibration absorption band of amide N–H bonding in the plane (Liu et al., 2023). The characteristic methylene deformation absorption band is observed at 1448 cm^{-1}, while the C–N bond stretching vibration absorption band is found at 1411 cm^{-1}. The band at 1347 cm^{-1} indicates the stretching vibration of C–N, and the band at 1311 cm^{-1} represents the amide III band, which arises from the coupling of N–H and C–N vibrations. The symmetric stretching absorption characteristic band of the C–O–C bond is observed at 1189 cm^{-1}, and the in-plane deformation vibrational absorption band of $–NH_2$ occurs at 1124 cm^{-1} (Wang et al., 2025). The band at 1059 cm^{-1} is attributed to the N–H in-plane deformation vibration, while the band at 946 cm^{-1} corresponds to the C–N stretching vibration and the out-of-plane deformation vibration of OH···O=. Analysis of the FTIR spectra reveals that SDGP contains functional groups such as amide and ester groups. The SDGP containing hydroxy acids exhibits narrow and sharp absorption bands for $\nu_{(N–H)}$ at 3423 cm^{-1} and $\nu_{(C=O)}$ at 1660 cm^{-1}. In contrast, SDGP without added hydroxy acids demonstrate a significant increase in the half-peak width of the spectral bands and a significant decrease in the intensity of the bands. This is due to the formation of hydrogen bonding between –CO–NH– and hydroxy acids. The SDGP with added tartaric acid shows the greatest intensity, indicating the strongest hydrogen bonding. Furthermore, the bands at 1347 and 1311 cm^{-1} are the characteristic bands of imide, and comparing the band intensities shows that the largest content of imide was found in SDGP with tartaric acid. The analysis of the FTIR spectra demonstrates that the introduction of hydroxy acids has increased the degree of imidization within the SDGP. These imides are generated through crosslinking between the amide groups on the polyacrylamide chain (Tang et al., 2016).

To clarify the effect of hydroxy acids on the structure of SDGP, XRD measurements were carried out. As illustrated in Fig. 2(b), SDGP exhibited two broad characteristic peaks at 23.1° and 37.5°, indicating that SDGP possesses an amorphous structure. The sharpest diffraction peak was observed in the SDGP containing tartaric acid, suggesting a strong interaction between tartaric acid and the polymer chains. Furthermore, the diffraction peaks at 2θ ~23.1° became sharper and more intense in the SDGP with hydroxy acid compared to the SDGP without hydroxy acid. This observation indicates that the addition of hydroxy acid enhances the orderliness and crosslinking of the polymer chains, leading to a more regular arrangement of the polymer chains.

The TG and DSC curves of SDGP are presented in Fig. 2(c) and (d). The TG curves exhibit similar shapes and can be categorized into three distinct stages. The first mass loss stage occurs between 50 and 193 °C, where the mass loss of SDGP is less than 10%, primarily due to the evaporation of water. The second mass loss stage takes place between 193 and 337 °C, during which SDGP begins to degrade as a result of the breakage of uncrosslinked polymer chains and the degradation of ester and amide groups (Cheng et al., 2023), resulting in a mass loss rate of about 20%. The third mass loss stage is observed between 337 and 600 °C, characterized by a sharp mass loss peak with the highest mass loss rate of 48.74%, mainly caused by the breakage of polymer main chains and the disruption of the crosslinking network structure. The crosslinking behavior of SDGP was investigated using DSC curves. As shown in Fig. 2(d), several distinct endothermic peaks appeared throughout

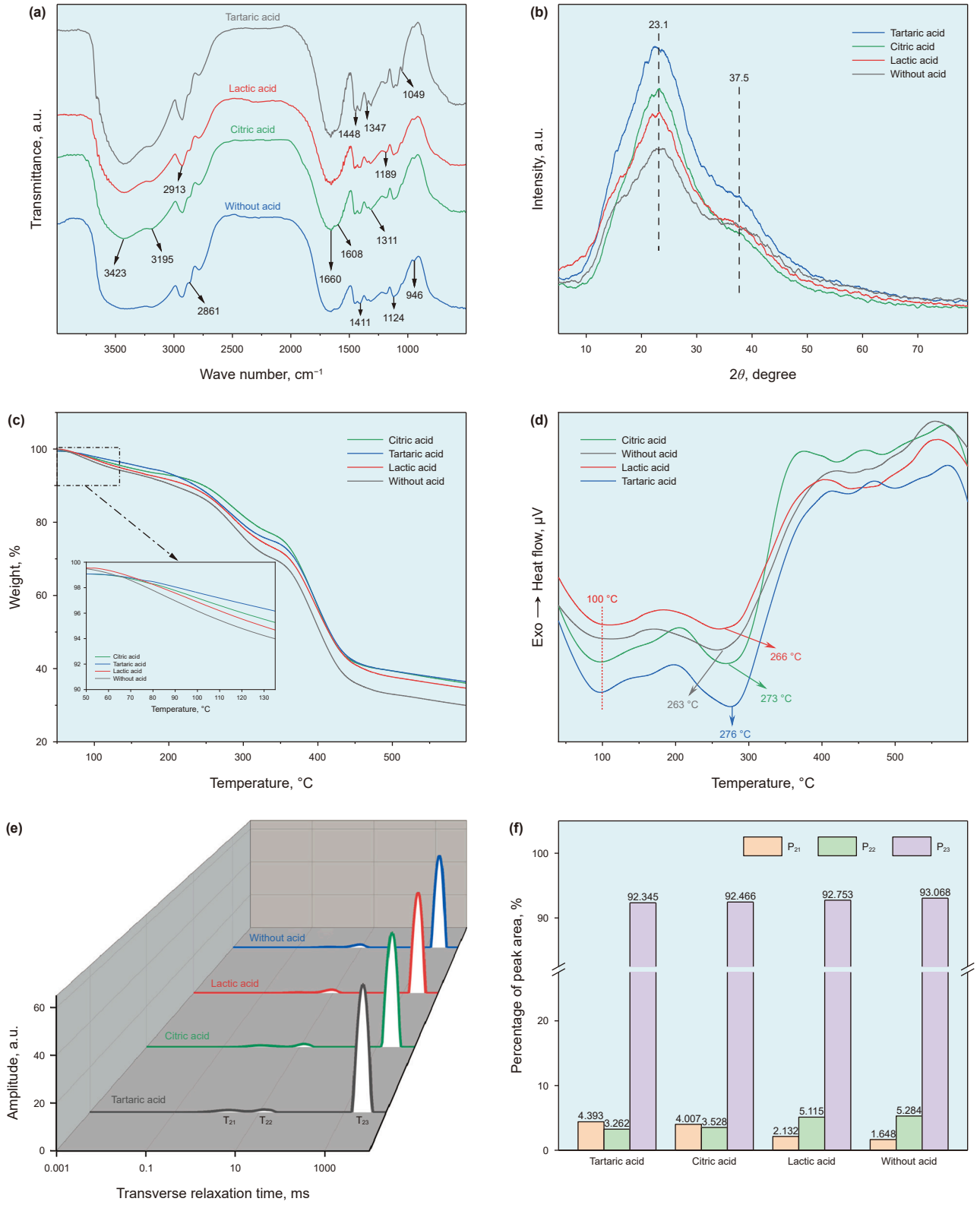

Fig. 2. (**a**) FTIR spectra of SDGP, (**b**) X-ray diffraction spectra of SDGP, (**c**) TG curves of the SDGP, (**d**) DSC curves of the SDGP, (**e**) the T_2 of water in SDGP containing different hydroxy acids measured by LF-NMR, (**f**) percentage of peak area in SDGP.

the heating process. In particular, the endothermic peak observed in the 220–280 °C range is attributed to the breakdown of uncrosslinked polyacrylamide side chains. A comparison of the decomposition temperatures of four different SDGPs within this temperature range indicates that the introduction of hydroxy acids shifted the endothermic peak to a higher temperature. This finding

suggests that hydroxy acids enhance the crosslinking density within the SDGP, effectively improving its structural stability and thermal resistance.

The surface morphology of SDGP was observed using SEM. It can be seen from Fig. 3 that SDGP formed three-dimensional networks. Crosslinkers make the polymer chains interlinked to form a mesh, resulting in a networked structure (Ren et al., 2021). As can be seen in Fig. 3(a), the internal network structure of SDGP without hydroxy acids appears relatively sparse and irregular, with thin interlayer walls. In contrast, Fig. 3(b)–(d) demonstrate that the three-dimensional network structure of SDGP containing hydroxy acids is more compact and regular, with thicker interlayer walls. Notably, the SDGP with tartaric acid exhibited the densest structure, suggesting enhanced internal hydrogen-bond interactions. These phenomena indicate that the introduction of hydroxy acids has increased the interaction force between the three-dimensional grids, which improved the structural stability of the SDGP.

The transverse relaxation time (T_2) spectra of SDGP are illustrated in Fig. 2(e), showing three peaks within the range of 0.01–10,000 ms. Based on the mobility of water, it can be roughly categorized: the components with T_2 between 1000 and 10,000 ms are highly mobile and were called free water. Free water is not attached to the polymer chain which can diffuse freely in the gel. Components with T_2 values less than 5 ms represent bound water, which exhibits poor mobility due to its binding to the gel matrix through hydrogen bonding with amide and carboxyl groups. In addition to these are the intermediate water (Vernáez et al., 2016; Zhu et al., 2021). The variation of T_2 and relative content of different states of water are depicted in Fig. 2(f). P_{21}, P_{22} and P_{23} represent the percentage of the corresponding peak areas of bound, intermediate, and free water, respectively. The peak area reflects the content of water. The percentage of bound water peak area in SDGP increased after the introduction of hydroxy acids, while the percentage of free water peak area decreased. This indicates that the addition of hydroxy acids increased the content of bound water and reduced the content of free water within the SDGP (Ji et al., 2024). This effect is attributed to hydroxy acids forming hydrogen bonds with water molecules, converting them into bound water and restricting their mobility. Additionally, the SEM results indicated that the SDGP with hydroxy acids have a denser network structure, leading to a restriction on the movement of free water. The restricted mobility of free water, which in turn reduced the probability of its collision with the ester group, led to a decrease in the hydrolysis of the crosslinker PEGDA.

3.2. Degradation properties of SDGP

It can be observed in Fig. 4(a) that SDGP exhibited high gel strength, which facilitated its ability to seal formation pressure. The gelation and degradation times of four SDGPs are shown in Fig. 4(b). The gelation time for the gel plugs was around 1 h. The degradation time of SDGP without acid (pH = 7) was 53 h. The incorporation of hydroxy acids extended the degradation time of SDGP. Specifically, the degradation time for SDGP with tartaric acid

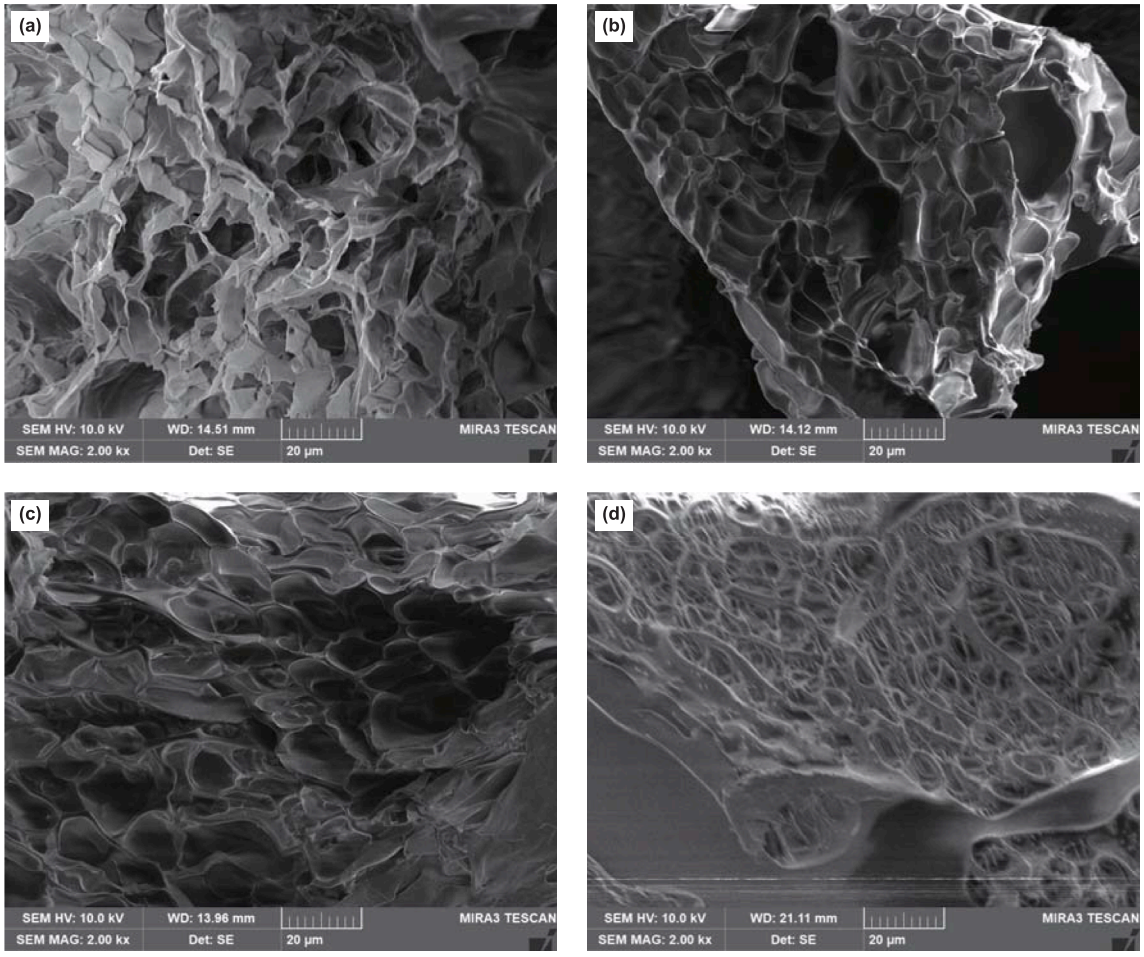

Fig. 3. SEM images of SDGP: **(a)** without acid, **(b)** lactic acid, **(c)** citric acid, **(d)** tartaric acid.

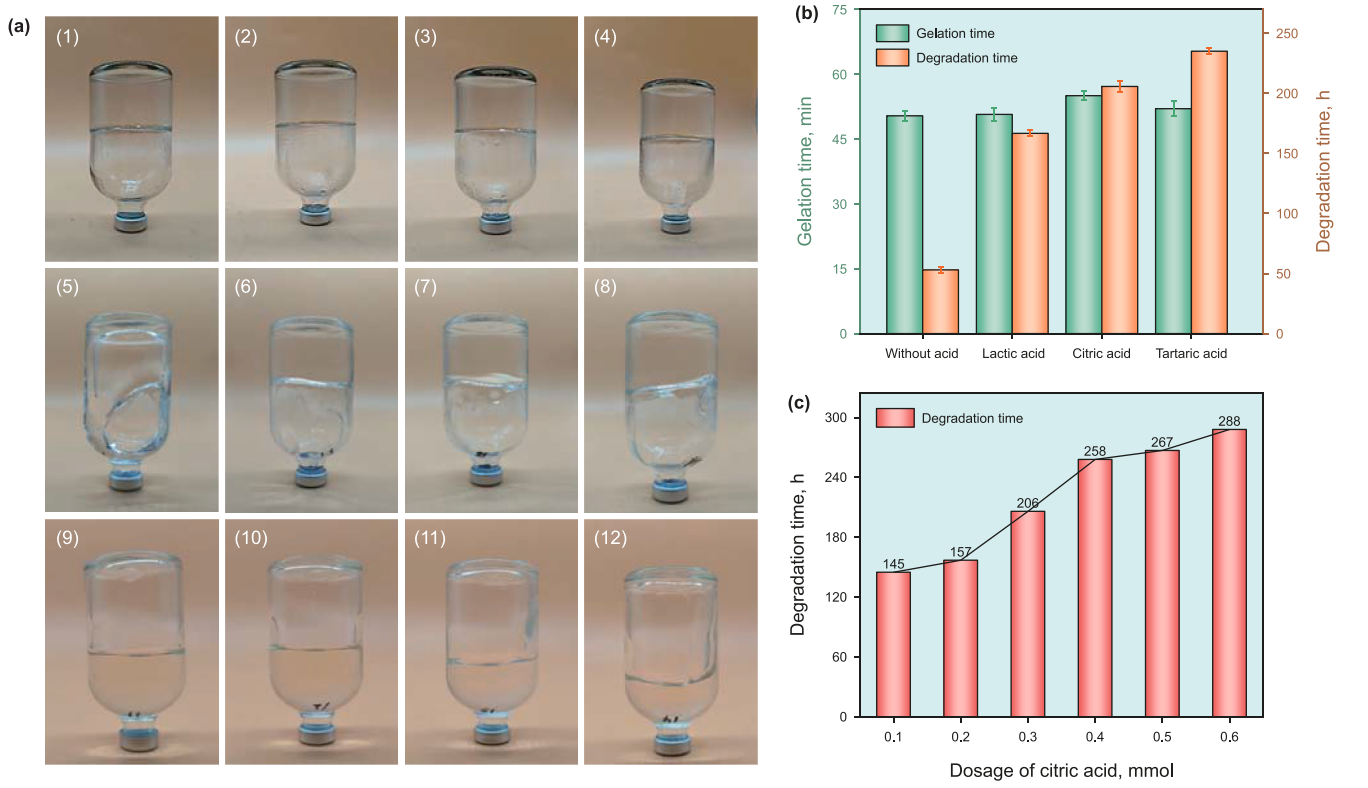

Fig. 4. **(a)** The physical pictures of SDGP at various stages: (1)–(4) after gelation; (5)–(8) after being placed at 90 °C for 48 h; (9)–(12) after complete degradation; (1, 5, 9) without acid; (2, 6, 10) lactic acid; (3, 7, 11) citric acid; (4, 8, 12) tartaric acid, **(b)** the gelation time and degradation time of SDGP, **(c)** the degradation time of SDGP with different concentration of citric acid.

(pH = 3) was 235 h, with citric acid (pH = 4) was 206 h, and with lactic acid (pH = 6) was 167 h. The degradation time of SDGP with hydroxy acids was significantly prolonged. This phenomenon can likely be attributed to the reaction of the amide groups within the polyacrylamide under temperature and acidic conditions, resulting in the formation of imides that crosslinked the polyacrylamide chains (Alavarse et al., 2022; Ding et al., 2015). This increase in crosslink density enhances the system's structural integrity. The elevated crosslinking density results in denser network structures, which consequently reduces the mobility of water within the gel, slows down the chain kinetics (Shen et al., 2019), and prolongs the degradation time. Furthermore, the amide groups can form hydrogen bonds with hydroxy acids, which strengthens the intermolecular forces between the polymer chains. Tartaric acid having the lowest pKa_1 value among the three hydroxy acids, proved to be the most effective in extending the degradation time of SDGP. The influence of hydroxy acid concentration on the degradation time of SDGP was further investigated. As shown in Fig. 4(c), increasing the concentration of citric acid from 0.1 to 0.6 mmol extended the degradation time of SDGP by 143 h (approximately 6 days). Chemical gels employed in oilfield operations for pressurized applications typically require high strength maintenance for a duration of 5–10 days. Based on the experimental results, it is evident that varying both the type and concentration of hydroxy acid can effectively regulate the degradation time of SDGP.

To avoid interfering with subsequent oil and gas exploitation, gel plugs need to be broken down after completing the pressure sealing operation. The SDGP gradually self-degradation after maintaining high strength for a period, eventually turning into a liquid. The viscosity of the residual liquid was tested, as shown in Fig. 5(a). The viscosity of the residual liquid from the SDGP without acid was measured at 115.37 mPa·s. In contrast, the viscosity of the residual liquid from the SDGP with hydroxy acids was higher, likely due to the enhanced formation of hydrogen bonds among the internal molecules. The SDGP can degrade into a viscous liquid, thereby eliminating the necessity for subsequent breaking operations.

Fig. 6 demonstrates the morphology of the SDGP after degradation. The degraded SDGP exhibited a layered folded structure or an irregular structure. The monomers were polymerized through free radical polymerization, forming a three-dimensional network structure under the crosslinking effect of PEGDA. Previous studies have shown that PEGDA, serving as a degradation crosslinker, contains internal ester groups that hydrolyze under temperature influence (Stillman et al., 2020; Zhang et al., 2022). Over time, the ester groups in PEGDA gradually hydrolyze, leading to the breakdown of crosslinking points and the collapse of the three-dimensional network structure. SDGP gradually transforming from a viscoelastic solid into a flowing polymer solution. A small amount of network structure can still be observed in Fig. 6(c), which is the reason why the degraded residual liquid of SDGP with viscosity (Zou et al., 2023).

3.3. *Mechanical properties and pressure resistance properties of SDGP*

The stretching properties of SDGP were evaluated due to the high requirements for gel strength and mechanical properties when sealing off formation pressure. The physical picture of the SDGP during the tensile test is shown in Fig. 5(b), while the results of the tensile test for the SDGP are presented in Fig. 5(c). The

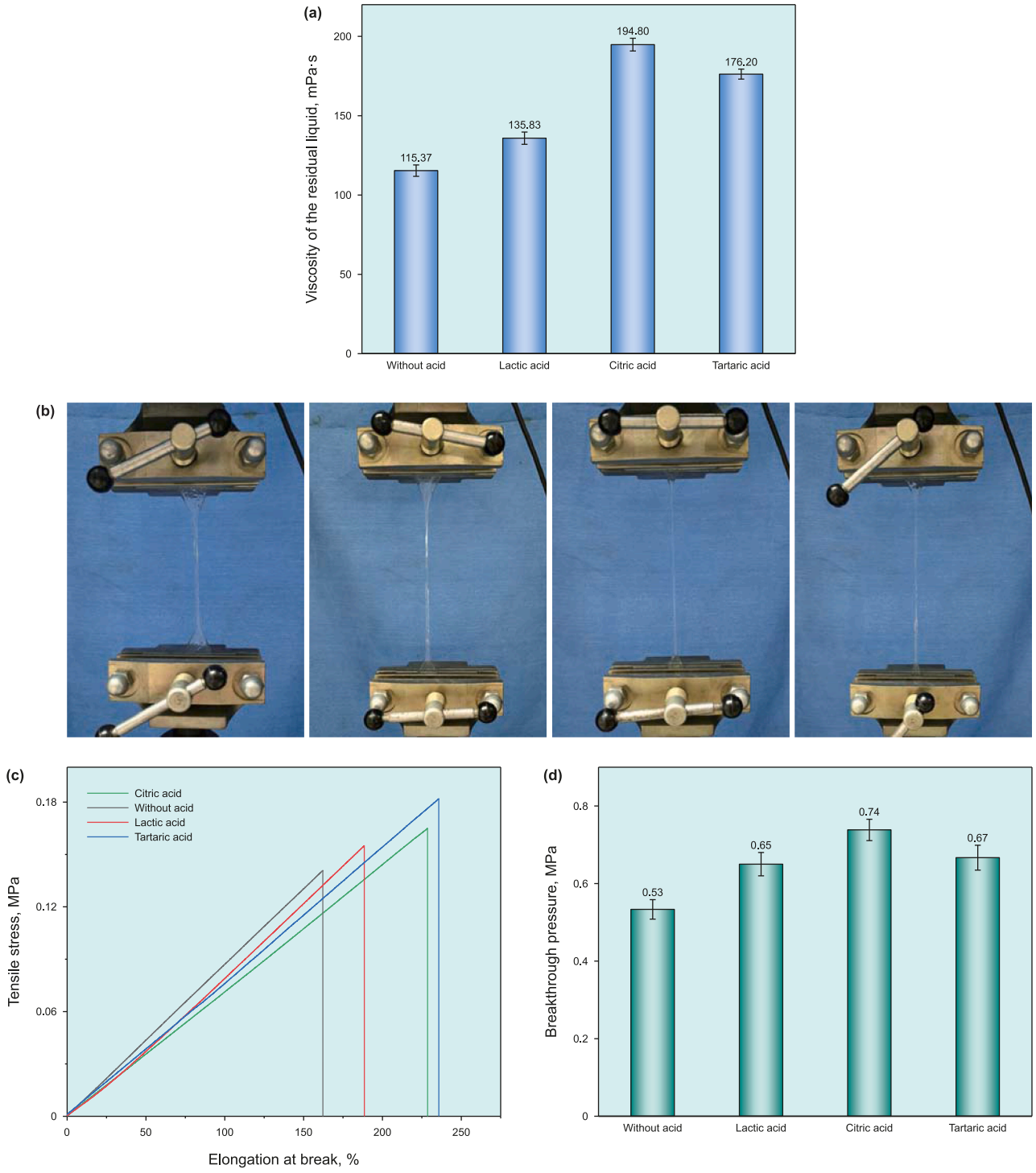

Fig. 5. **(a)** The viscosity test results of degraded residual liquid, **(b)** physical drawing of tensile test of SDGP, **(c)** stress-strain curves of tensile test for SDGP, **(d)** pressure resistance test results for SDGP.

elongation at break and stress of SDGP increased with the addition of hydroxy acids. For the SDGP without acid, the elongation at break was 162.18%, with a stress of 0.141 MPa. For the SDGP with tartaric acid, the elongation increased to 235.75% for elongation at break and 0.182 MPa for stress. In polymer gel systems, crosslink density significantly impacts the mechanical properties of the gel (Shen et al., 2019). The tensile properties of SDGP with hydroxy acids were generally improved compared to those without. The results suggest that the introduction of hydroxy acids altered the crosslinking within the SDGP.

Pressure resistance is a critical parameter for assessing the performance of pressure-controlled plugging gels. A higher-pressure resistance indicates a greater ability to seal off pressure. The pressure resistance performance of SDGP was evaluated by

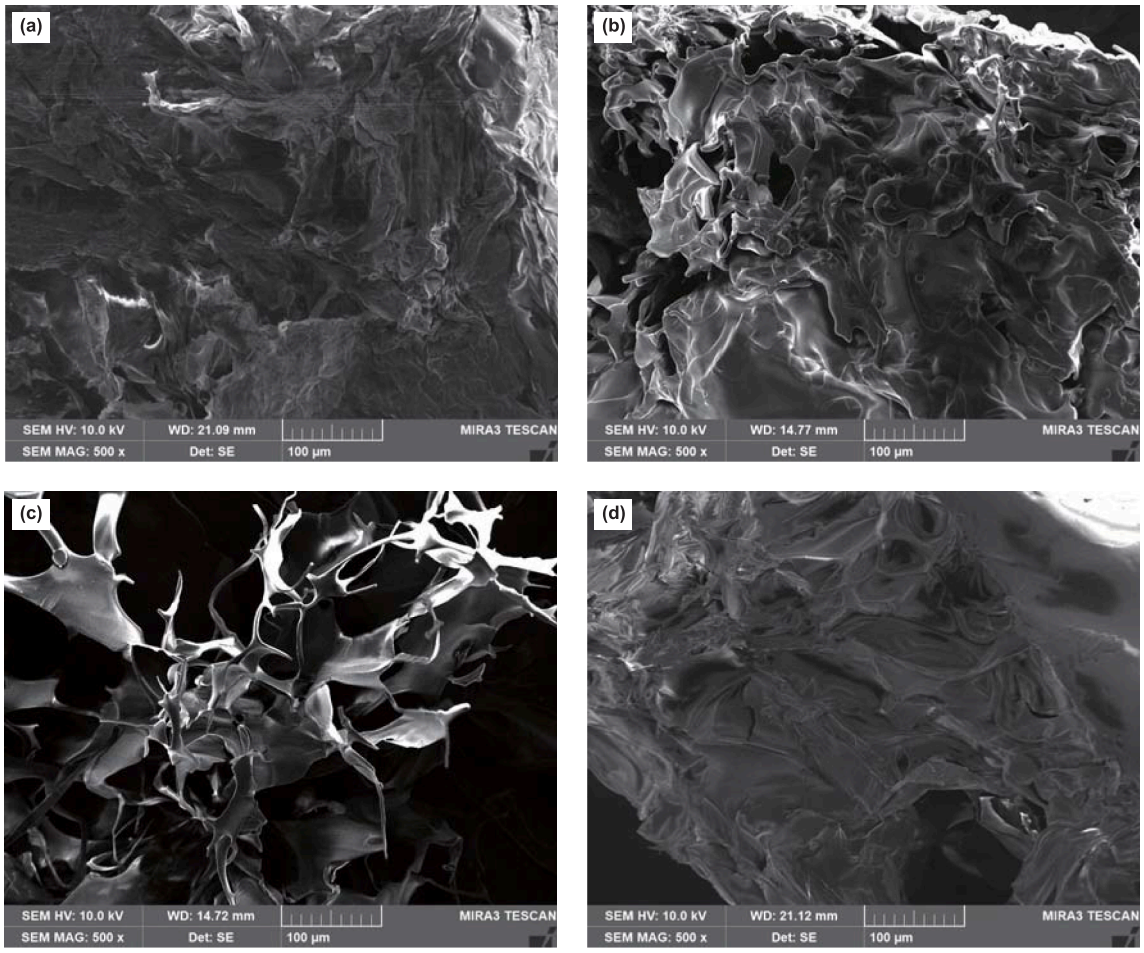

Fig. 6. Morphology of the SDGP after degradation: **(a)** without acid, **(b)** lactic acid, **(c)** citric acid, **(d)** tartaric acid.

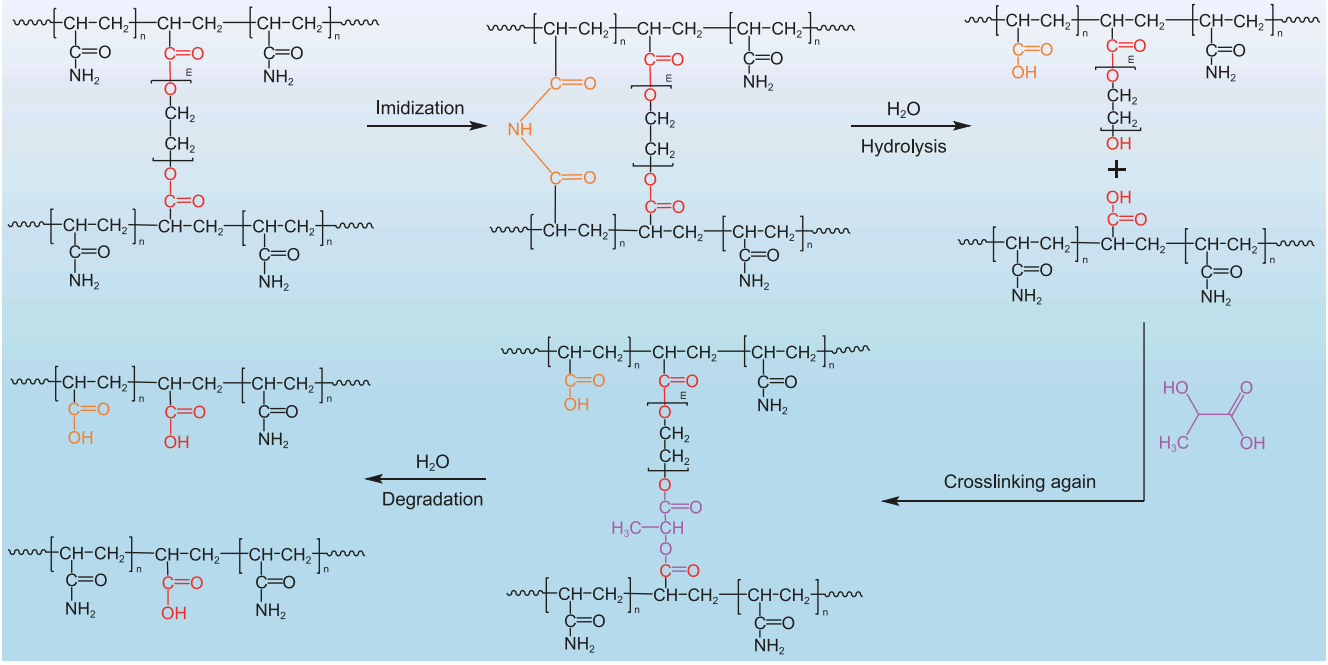

Fig. 7. Schematic diagram of the mechanism of lactic acid regulation of SDGP degradation time.

measuring the breakthrough pressure, with the experimental results presented in Fig. 5(d). The breakthrough pressure of the SDGP without acid was 0.53 MPa. The breakthrough pressure for SDGP with citric acid was 0.74 MPa. The pressure resistance of the SDGP was improved with the addition of hydroxy acids. The results of the tensile and pressure resistance tests indicate that the addition of hydroxy acids not only successfully regulated the degradation time of SDGP but also did not compromise its properties. In fact, the introduction of hydroxy acids enhanced the performance of the SDGP.

3.4. The possible mechanism of SDGP degradation time regulation

A comprehensive analysis of the above results elucidated the effect of hydroxy acids on the degradation time of SDGP. Fig. 7 illustrates the mechanism by lactic acid regulated the degradation time of SDGP. XRD results show that the introduction of hydroxyl acid increases the degree of crosslinking in SDGP. SEM images revealed that the three-dimensional network structure of SDGP containing hydroxy acids was denser and the interlayer walls became thicker, which indirectly proved that the crosslinking density inside SDGP increased. LF-NMR results showed that the content of bound water inside SDGP increased and the content of free water decreased after the addition of hydroxy acids. Hydroxy acids contained hydroxyl and carboxyl groups that can form hydrogen bonding interactions with water inside SDGP as well as with amide groups on the molecular chain, and some of the free water movement is limited, leading to a slowing of the hydrolysis of the crosslinker PEGDA. Among the three hydroxy acids, lactic acid ($pKa_1 = 3.86$), tartaric acid ($pKa_1 = 2.98$), and citric acid ($pKa_1 = 3.13$), tartaric acid is more acidic and has the most obvious effect on the extension of the degradation time of SDGP. Stronger acidity favors the crosslinking reaction between polyacrylamide chains, generating imide and increasing the crosslink density of SDGP. The increased crosslink density results in a denser three-dimensional network structure, which compresses the space for water molecules inside the gel. This reduction in free water molecules slows the hydrolysis of ester groups, thereby prolonging the degradation time of SDGP. Additionally, when the ester groups in the crosslinker PEGDA hydrolyze, the polymer chains contain carboxyl and hydroxyl groups. In the gel system (with a water content >90%), the presence of water causes a significant leftward shift in the esterification equilibrium constant, making it difficult to reconnect the linear polyacrylamide molecular chains directly through the functional groups on the polymer chains. After introducing hydroxy acids, under the catalytic action of acids, the hydroxyl and carboxyl groups on the hydroxy acids react with the carboxyl and hydroxyl groups on the polyacrylamide chains, which again crosslinks the polymer chains and achieves controlled degradation of SDGP.

4. Conclusions

This study regulates the degradation time of the gel plug by introducing hydroxy acids, which alter the crosslinking density between polymer chains. The following conclusions can be drawn:

(1) The controlled degradation of SDGP is achieved by adjusting the crosslinking density through the use of hydroxy acids.
(2) The degradation times of SDGP were observed to be 53 h without acid, 167 h with lactic acid, 206 h with citric acid, and 235 h with tartaric acid.
(3) The breakthrough pressure of SDGP without acid was measured at 0.53 MPa, whereas that of the SDGP with citric acid was found to be 0.74 MPa. The inclusion of hydroxy acids not only regulated the degradation time of SDGP but also enhanced its mechanical properties.
(4) Hydroxy acids act as crosslinkers in the regulation of the degradation time of SDGP, with both hydroxyl and carboxyl groups functioning synergistically.

CRediT authorship contribution statement

Ren-Jing Ji: Writing – original draft, Visualization, Methodology, Data curation, Conceptualization. **Xiao-Rong Yu:** Writing – review & editing, Methodology, Funding acquisition, Conceptualization. **Zhi-Xiang Xu:** Writing – review & editing, Formal analysis, Conceptualization. **Xian-Qun Wang:** Visualization, Supervision, Data curation. **Jia-Yu Tan:** Supervision, Data curation. **Yong-Quan Han:** Visualization, Formal analysis. **Huan Yang:** Validation, Formal analysis. **Gao-Shen Su:** Visualization, Investigation.

Data availability

Data will be made available on request.

Declaration of interest statement

The authors declare that they have no known competing financial interests or personal relationships that could have appeared to influence the work reported in this paper.

Acknowledgments

This research was funded by the Open Fund for State Key Laboratory of Shale Oil and Gas Enrichment Mechanisms and Effective Development, grant number (35800000-22-ZC0609-0017).

References

Alavarse, A.C., Frachini, E.C.G., da Silva, R.L.C.G., Lima, V.H., Shavandi, A., Petri, D.F.S., 2022. Crosslinkers for polysaccharides and proteins: Synthesis conditions, mechanisms, and crosslinking efficiency, a review. Int. J. Biol. Macromol. 202, 558–596. https://doi.org/10.1016/j.ijbiomac.2022.01.029.

Bai, Y., Liu, C., Sun, J., Lv, K., 2022. Use of a polymer gel for killing a high-temperature and high-pressure gas well. SPE J. 27 (6), 3297–3313. https://doi.org/10.2118/210586-PA.

Burni, F.A., Xu, W., Spencer, R.G., Bergstrom, E., Chappell, D., Wee, J.K., Raghavan, S.R., 2024. Self-degrading molecular organogels: Self-assembled gels programmed to spontaneously liquefy after a set time. Adv. Funct. Mater. 34 (40), 2403617. https://doi.org/10.1002/adfm.202403617.

Chen, C., Lei, Y., Liu, D., Yin, Y., Wang, T., Li, X., 2012. Application of smart packer technology in underbalanced completion. In: IADC/SPE Asia Pacific Drilling Technology Conference and Exhibition. https://doi.org/10.2118/155888-MS.

Cheng, J., Yang, H., Gao, J., Gu, X., Yu, X., Su, G., Jiang, Z., Zhu, Y., 2023. Synthesis and molecular dynamics simulation of amphoteric hydrophobically associating polymer. J. Mol. Liq. 388, 122751. https://doi.org/10.1016/j.molliq.2023.122751.

Cheng, L., Qin, Y., Su, Y., Pan, Y., Wang, Y., Liao, R., Li, Z., 2022. Development of a high-strength and adhesive polyacrylamide gel for well plugging. ACS Omega 7 (7), 6151–6159. https://doi.org/10.1021/acsomega.1c06626.

Ding, H., Tang, H., Wang, F., Zhang, H., Guo, Y., 2015. The molecular structure control of butyl methacrylate/acrylamide (co)polymers. Mater. Des. 88, 820–826. https://doi.org/10.1016/j.matdes.2015.09.037.

Du, L., Xiao, Y.Y., Jiang, Z.C., Xu, H., Zeng, H., Li, H., 2025. A high temperature-resistant, strong, and self-healing double-network hydrogel for profile control in oil recovery. J. Colloid Interface Sci. 679 (Part B), 490–502. https://doi.org/10.1016/j.jcis.2024.10.077.

Ji, R., Yu, X., Yang, H., Wang, X., Su, G., 2024. Preparation and degradable mechanism of self-breaking gel valve for underbalanced drilling. Geoenergy Sci. Eng. 235, 212705. https://doi.org/10.1016/j.geoen.2024.212705.

Jia, H., Chen, H., Zhao, J.Z., 2020. Development of a highly elastic composite gel through novel intercalated crosslinking method for wellbore temporary plugging in high-temperature reservoirs. SPE J. 25 (6), 2853–2866. https://doi.org/10.2118/201090-PA.

Jia, H., Kang, Z., Zhu, J., Ren, L., Cai, M., Wang, T., Xu, Y., Li, Z., 2021. High density bromide-based nanocomposite gel for temporary plugging in fractured reservoirs with multi-pressure systems. J. Pet. Sci. Eng. 205, 108778. https://doi.org/10.1016/j.petrol.2021.108778.

Kang, Z., Jia, H., Li, Z.G., Xia, B., Wang, Y., Jiang, Y., Peng, H.L., 2023. Comprehensive evaluation of chemical breakers for multistage network ultra-high strength gel. Pet. Sci. 20 (5), 2864–2878. https://doi.org/10.1016/j.petsci.2023.05.001.

Kang, Z., Liu, Y.T., Jia, H., Xia, B., Ou, H.M., Pu, Q.B., Hussein, I.A., 2024. Progress and prospects of in situ polymer gels for sealing operation in wellbore and near-well zone. Energy & Fuels 38 (5), 3539–3563. https://doi.org/10.1021/acs.energyfuels.3c04382.

Li, Z., Li, X., Du, K., Liu, H., 2020. Development of a new high-temperature and high-strength polymer gel for plugging fractured reservoirs. Upstream Oil Gas Technol. 5, 100014. https://doi.org/10.1016/j.upstre.2020.100014.

Li, Z., Wang, S., Tao, Y., Ma, H., Wu, J., 2018. Research and application of the HTHS anti-H_2S gel valve for underbalanced drilling. J. Pet. Sci. Eng. 164, 174–181. https://doi.org/10.1016/j.petrol.2018.01.038.

Liu, J., Fu, H., Luo, Z., Chen, W., Liu, F., Zhao, M., 2023. Preparation and performance of pH-temperature responsive low-damage gel temporary plugging agent. Colloids Surf. A Physicochem. Eng. Asp. 662, 130990. https://doi.org/10.1016/j.colsurfa.2023.130990.

Liu, J., Huang, X.F., Lu, L.J., Xu, J.C., Wen, Y., Yang, D.H., Zhou, Q., 2010. Optimization of biodemulsifier production from *Alcaligenes* sp. S-XJ-1 and its application in breaking crude oil emulsion. J. Hazard Mater. 183 (1–3), 466–473. https://doi.org/10.1016/j.jhazmat.2010.07.047.

Liu, Z., Xu, J., Peng, W., Yu, X., Chen, J., 2023. The development and deployment of degradable temporary plugging material for ultra-deepwater wells. Processes 11 (6), 1685. https://doi.org/10.3390/pr11061685.

Mardashov, D.V., Rogachev, M.K., Zeigman, Y.V., Mukhametshin, V.V., 2021. Well killing technology before workover operation in complicated conditions. Energies 14 (3), 654. https://doi.org/10.3390/en14030654.

Ramanathan, R., Nasr-El-Din, H.A., 2021. A comparative experimental study of alternative iron sulfide scale dissolvers in the presence of oilfield conditions and evaluation of new synergists to aminopolycarboxylic acids. SPE J. 26 (2), 693–715. https://doi.org/10.2118/205005-PA.

Ren, Y., Sun, X., Chen, L., Li, Y., Sun, M., Duan, X., Liang, W., 2021. Structures and impact strength variation of chemically crosslinked high-density polyethylene: effect of crosslinking density. RSC Adv. 11 (12), 6791–6797. https://doi.org/10.1039/D0RA10365A.

Shen, J., Lin, X., Liu, J., Li, X., 2019. Effects of cross-link density and distribution on static and dynamic properties of chemically cross-linked polymers. Macromolecules 52 (1), 121–134. https://doi.org/10.1021/acs.macromol.8b01389.

Shu, Z., Qi, Y., Luo, P., 2023. Research and performance evaluation of modified nano-silica gel plugging agent. J. Appl. Polym. Sci. 140 (21). https://doi.org/10.1002/app.53873.

Song, T., Bai, B., Eriyagama, Y., Schuman, T., 2023. Lysine crosslinked polyacrylamide–A novel green polymer gel for preferential flow control. ACS Appl. Mater. Interfaces 15 (3), 4419–4429. https://doi.org/10.1021/acsami.2c17390.

Stillman, Z., Jarai, B.M., Raman, N., Patel, P., Fromen, C.A., 2020. Degradation profiles of poly(ethylene glycol)diacrylate (PEGDA)-based hydrogel nanoparticles. Polym. Chem. 11 (2), 568–580. https://doi.org/10.1039/C9PY01206K.

Sydansk, R.D., 1990. A newly developed chromium(lll) gel technology. SPE Reserv. Eng. 5 (3), 346–352. https://doi.org/10.2118/19308-PA.

Tang, H., Wei, F., Ding, H., 2016. Transformation of the molecular structure of butyl methacrylate/acrylamide/acrylic acid copolymers during heat treatment. Mater. Des. 96, 304–313. https://doi.org/10.1016/j.matdes.2016.02.014.

Vernáez, O., Dagreou, S., Grassl, B., Müller, A.J., 2016. Dynamic rheology and relaxation time spectra of oil-based self-degradable gels. J. Polym. Sci. B Polym. Phys. 54 (3), 433–444. https://doi.org/10.1002/polb.23918.

Wang, G., He, S., Yu, J., Liu, L., Wang, T., Lai, L., 2024. In-situ poly(hexahydrotriazine) gels temporary plugging agent suitable for high-temperature reservoirs: regulation by inorganic chloride salts. Geoenergy Sci. Eng. 239, 212905. https://doi.org/10.1016/j.geoen.2024.212905.

Wang, K., Liu, G., Guo, Y., Yang, H., Chen, Z., Su, G., Wang, Y., Wei, B., Yu, X., 2022. Preparation and properties of degradable hydrogels as a temporary plugging agent used for acidizing treatments to enhance oil recovery. Colloids Surf. A Physicochem. Eng. Asp. 637, 128218. https://doi.org/10.1016/j.colsurfa.2021.128218.

Wang, K., Wang, S., Wang, X.Y., Wang, X.Q., Zheng, L., Wen, J., Yang, H., Zhang, H., 2025. Modulation of syneresis rate and gel strength of PAM-PEI gels by nanosheets and their mechanisms. Colloids Surf. A Physicochem. Eng. Asp. 704, 135525. https://doi.org/10.1016/j.colsurfa.2024.135525.

Wang, Y., Liu, D., Liao, R., Zhang, G., Zhang, M., Li, X., 2022. Study of adhesive self-degrading gel for wellbore sealing. Colloids Surf. A Physicochem. Eng. Asp. 651, 129567. https://doi.org/10.1016/j.colsurfa.2022.129567.

Xu, H., Zhang, L., Wang, J., Jiang, H., 2023. Evaluation of self-degradation and plugging performance of temperature-controlled degradable polymer temporary plugging agent. Polymers 15 (18), 3732. https://doi.org/10.3390/polym15183732.

Xu, Z., Zhao, M., Yang, Z., Wang, P., Liu, J., Xie, Y., Wu, Y., Gao, M., Li, L., Song, X., Dai, C., 2024. Novel mussel-inspired high-temperature resistant gel with delayed crosslinking property for ultra-deep reservoir fracturing. Adv. Funct. Mater. 34 (42), 2405111. https://doi.org/10.1002/adfm.202405111.

Yang, F., Li, F., Ji, R., Yu, X., Yang, H., Su, G., 2024a. Self-degradable rubber plug for temporary plugging and its degradation mechanism. Gels 10 (10), 615. https://doi.org/10.3390/gels10100615.

Yang, F., Liu, J., Ji, R., Yu, X., Yang, H., Su, G., 2024b. Degradable gel for temporary plugging in high temperature reservoir and its properties. Gels 10 (7), 445. https://doi.org/10.3390/gels10070445.

Yang, H.Y., Li, Y.R., Wei, W., Liu, X.H., 2023. Preparation and application of new polycarboxylic acid for scale inhibition. J. Phys. Conf. Ser. 2430, 012020. https://doi.org/10.1088/1742-6596/2430/1/012020.

Yin, H., Yin, X., Cao, R., Zeng, P., Wang, J., Wu, D., Luo, X., Zhu, Y., Zheng, Z., Feng, Y., 2022. In situ crosslinked weak gels with ultralong and tunable gelation times for improving oil recovery. Chem. Eng. J. 432, 134350. https://doi.org/10.1016/j.cej.2021.134350.

Ying, X., Yuan, X., Yadong, Z., Ziyi, F., 2021. Study of gel plug for temporary blocking and well-killing technology in low-pressure, leakage-prone gas well. SPE Prod. Oper. 36 (1), 234–244. https://doi.org/10.2118/204213-PA.

Zhang, H.J., Zhu, D.Y., Gong, Y.L., Qin, J.H., Liu, X.N., Pi, Y.H., Zhao, Q., Luo, R.T., Wang, W.S., Zhi, K.K., Mu, Z.J., 2022. Degradable preformed particle gel as temporary plugging agent for low-temperature unconventional petroleum reservoirs: effect of molecular weight of the cross-linking agent. Pet. Sci. 19 (6), 3182–3193. https://doi.org/10.1016/j.petsci.2022.07.013.

Zhou, S., Qi, N., Zhang, Z., Jiang, P., Li, A., Lu, Y., Su, X., 2025. Recent progress in intrinsic self-healing polymer materials: mechanisms, challenges and potential applications in oil and gas development. Chem. Eng. J. 511, 161906. https://doi.org/10.1016/j.cej.2025.161906.

Zhu, D.Y., Deng, Z.H., Chen, S.W., 2021. A review of nuclear magnetic resonance (NMR) technology applied in the characterization of polymer gels for petroleum reservoir conformance control. Pet. Sci. 18 (6), 1760–1775. https://doi.org/10.1016/j.petsci.2021.09.008.

Ziad, A. Bin, Gromakovskii, D., Al-Sagr, A., Al-Driweesh, S., 2016. First successful application of temporary gel plug replacing calcium carbonate chips to isolate depleted reservoir, case study from Saudi Arabia gas field. In: Day 2 Thu. SPE. https://doi.org/10.2118/178986-MS.

Zou, C., Dai, C., Liu, Y., You, Q., Ding, F., Huang, Y., Sun, N., 2023. A novel self-degradable gel (SDG) as liquid temporary plugging agent for high-temperature reservoirs. J. Mol. Liq. 386, 122463. https://doi.org/10.1016/j.molliq.2023.122463.